

Inclusive J Production in Z^0 Decays

The L3 Collaboration

ABSTRACT

Inclusive J production in Z^0 decays is observed via the leptonic decay mode $J \rightarrow \ell^+ \ell^-$ ($\ell = e, \mu$). We measure the branching ratio $\text{Br}(Z^0 \rightarrow J + X) = (4.1 \pm 0.7 \text{ (stat.)} \pm 0.3 \text{ (sys.)}) \times 10^{-3}$. We have calculated the fraction of the J mesons from b-hadron decay and find a branching ratio of $\text{Br}(b \rightarrow J + X) = (1.3 \pm 0.2 \text{ (stat.)} \pm 0.2 \text{ (sys.)}) \times 10^{-2}$. We determine the average fractional energy of bottom hadrons $\langle x_E \rangle = 0.70 \pm 0.03 \text{ (stat.)}_{-0.01}^{+0.02} \text{ (sys.)}$ using the momentum spectrum of the J mesons. From a study of the angle between the J and the most energetic jet, we set an upper limit on the branching ratio $\text{Br}(Z^0 \rightarrow q\bar{q}g^*; g^* \rightarrow J + X) < 7.0 \times 10^{-4}$ at 90% confidence level.

(Submitted to Phys. Lett. B)

1 Introduction

The dominant mechanism for the production of J mesons in Z^0 decays is expected to be:

$$e^+e^- \rightarrow Z^0 \rightarrow b\bar{b}; \quad b(\bar{b}) \rightarrow J + X. \quad (1)$$

This is illustrated in Figure 1a. The latter decay proceeds mainly through a ‘‘colour-suppressed’’ spectator diagram, in which the c and \bar{c} have to match in colour. However, the magnitude of this colour suppression can be reduced by QCD effects, which leads to a considerable change in the inclusive branching ratio [1]. The decay $b \rightarrow J + X$ has also been suggested [2] as a favourable mode to tag b-hadrons¹. Measurements of $\text{Br}(b \rightarrow J + X)$ have been performed by experiments at CESR and DORIS [3] for B-mesons produced at the $\Upsilon(4S)$. Recently, a measurement of $\text{Br}(Z^0 \rightarrow J + X)$ has been reported at LEP energies [4].

The J momentum in b-hadron decays is strongly correlated with the parent particle momentum, which is sensitive to the fragmentation of the b-quark. This allows us to determine the b-quark fragmentation parameter using the measured J momentum distribution.

In addition to process (1), at LEP energies the J meson can also be produced from gluon jets:

$$e^+e^- \rightarrow Z^0 \rightarrow q\bar{q}g^*; \quad g^* \rightarrow J + X. \quad (2)$$

The dominant diagram is illustrated in Figure 1b. An estimate of this rate was first made more than a decade ago [5]. Recently, a new calculation has been performed [6]. The calculated rate is 2.3×10^{-4} , but has a theoretical uncertainty of at least a factor of two. Studies of the process (2) give information on the interplay between the non-perturbative and perturbative effects in QCD. In order to produce a J meson, the gluon bremsstrahlung must be hard. Therefore, the J mesons from this process are expected to be produced at large angles with respect to the most energetic quark [6]. The production rate of J mesons via other processes is predicted [7] to be smaller than 10^{-5} , and is not considered in this analysis.

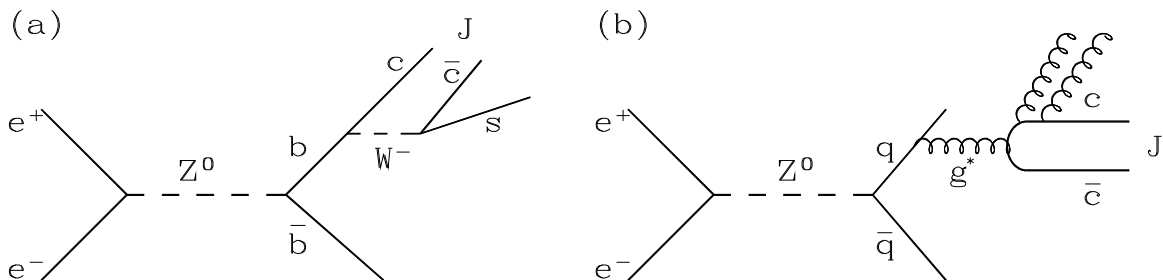


Figure 1: Diagrams for a) $e^+e^- \rightarrow Z^0 \rightarrow b\bar{b}$; $b(\bar{b}) \rightarrow J + X$; and b) $e^+e^- \rightarrow Z^0 \rightarrow q\bar{q}g^*$; $g^* \rightarrow J + X$.

J mesons are identified by their leptonic decay, $J \rightarrow \ell^+\ell^-$ ($\ell = e, \mu$). Inclusive leptons used in this analysis are selected from a sample of 410 000 $e^+e^- \rightarrow$ hadrons events, recorded in 1990 and 1991 with the L3 detector at $\sqrt{s} \approx m_Z$. The data sample corresponds to an integrated luminosity of 17.5 pb^{-1} .

¹In this paper, references to a specific charged state also imply the charged conjugate state.

2 The L3 Detector

The detector consists of a central tracking chamber, a high resolution electromagnetic calorimeter composed of BGO crystals, a cylindrical array of scintillation counters, a uranium and brass hadron calorimeter with proportional wire chamber readout, and a precise muon spectrometer. These detectors are installed in a 12 m diameter solenoid which provides a uniform field of 0.5 T along the beam direction. A detailed description of the L3 detector can be found elsewhere [8].

The central tracking chamber is a time expansion chamber (TEC) which consists of two cylinders, the inner and outer chambers, with 12 and 24 sectors, respectively. The R - ϕ coordinate of a track is measured with a maximum of 62 anode wires (8 in the inner chamber, 54 in the outer). The single wire resolution is $58 \mu\text{m}$ averaged over the entire cell and the double-track resolution is $640 \mu\text{m}$.

The fine segmentation of the electromagnetic and hadron calorimeters allows us to measure the direction of jets with an angular resolution of 2.1° , and to measure the total energy of hadronic events from Z^0 decay with a resolution of 10.2% [9]. The muon detector consists of three layers of precise drift chambers, which measure a muon trajectory 56 times in the bending plane, and 8 times in the non-bending direction. For this analysis, electrons are identified in the angular range $42^\circ < \vartheta < 138^\circ$, and muons in the range $36^\circ < \vartheta < 144^\circ$.

3 Identification of J Candidates

The trigger requirements and the selection criteria for hadronic events have been described in detail elsewhere [10]. Muons are identified and measured in the muon chamber system. We require that a muon track consists of track segments in at least two of the three layers of the muon chambers and that the muon track points to the interaction region. Electrons are identified by associating clusters of energy in the BGO calorimeter with charged tracks in the central tracking chamber. The lateral shower profile has to be consistent with the shape of an electromagnetic shower as determined from test beam studies. Furthermore, the track associated with the cluster should be separated from other tracks.

In the laboratory system, the J mesons often decay into one high and one low momentum lepton. We therefore select muons and electrons with a momentum larger than 2 GeV, rather than the usual 3 or 4 GeV criterion that we impose for other analyses [11], and place less stringent cuts on the shower shape for one of the electrons. We require the opening angle between two oppositely charged lepton candidates to be smaller than 90° .

Lepton pairs that pass the above cuts can also arise from several different background sources. The dominant source is the semileptonic decay of a b-hadron to a c-hadron, followed by the semileptonic decay of the c-hadron. Other sources are: a prompt lepton from a b- or c-hadron decay, with a misidentified hadron or a lepton from K or π decay; a misidentified hadron with a lepton from K or π decay; and two misidentified hadrons. All these processes tend to give masses well below that of the J meson.

4 Background Simulation and Acceptance Calculation

To simulate the background processes, we use 800 000 five flavour $Z^0 \rightarrow q\bar{q}$ Monte Carlo events produced using the JETSET model [12]. In addition, we generate 70 000 and 90 000 b-flavour

events, in which one of the b-quarks is forced to decay semileptonically into a μ or e, respectively. These are of particular relevance due to the dominant background coming from $Z^0 \rightarrow b\bar{b}$ events.

The events are passed through the full L3 detector simulation [13], which includes the effects of experimental resolution, energy loss, multiple scattering, interactions and decays in the detector materials. The Peterson fragmentation function [14] is used in the Monte Carlo simulation to describe the fragmentation of c- and b-quarks. The input fragmentation parameters used in the generator are: $\varepsilon_c^z = 0.07$ for c-quarks, found by extrapolation from PETRA and PEP data [15], and $\varepsilon_b^z = 0.008$ for b-quarks, taken from our own measurement [11]. We also use the L3 measurement of $\text{Br}(b \rightarrow \ell + X) = 0.119 \pm 0.003 \text{ (stat.)} \pm 0.006 \text{ (sys.)}$ [11] and take $\text{Br}(c \rightarrow \ell + X) = 0.096 \pm 0.006$ from measurements at PETRA and PEP [16].

The acceptance for $J \rightarrow \mu^+\mu^-$ is mainly determined by the angular coverage of the muon chambers and the absorption of low momentum muons in the calorimeter. The acceptance calculation was based on the fully simulated JETSET Monte Carlo b-flavour events, requiring the decay chain $b \rightarrow J + X; J \rightarrow \mu^+\mu^-$ for one of the b-hadrons. The acceptance for this process is calculated to be $0.28 \pm 0.01 \text{ (stat.)}$. The acceptance for $J \rightarrow e^+e^-$ is determined by the angular coverage of the BGO barrel electromagnetic calorimeter and the isolation requirements imposed by the electron selection criteria. The acceptance for $J \rightarrow e^+e^-$ coming from $b \rightarrow J + X$ is calculated to be $0.15 \pm 0.01 \text{ (stat.)}$.

The systematic error on the selection efficiencies is estimated by varying the cuts, in particular the momentum cut which is varied from 2 to 4 GeV. We also apply extra kinematic cuts, especially for the case when the two leptons are in different jets.

Inefficiencies in the TEC, BGO and muon chambers are not included in the Monte Carlo simulation. They are calculated using the data. Taking into account the correlations between the two leptons, the efficiency for finding the two muons is $\varepsilon_{\mu^+\mu^-} = 0.92 \pm 0.02 \text{ (stat.)}$ and for the two electrons is $\varepsilon_{e^+e^-} = 0.82 \pm 0.02 \text{ (stat.)}$.

J mesons can also result from the cascade decay of ψ 's and the radiative decay of χ_c 's produced in b-hadron decay [17]. From a Monte Carlo simulation, the effect of the cascade decays on the acceptance and the J momentum spectrum is negligible.

5 Determination of $\text{Br}(Z^0 \rightarrow J + X)$

The measured invariant mass distributions of the $\ell^+\ell^-$ pairs are shown in Figure 2. We fit the invariant mass distribution in the mass region $2.0 < m_{\ell^+\ell^-} < 4.0$ GeV with a Gaussian for the signal and a polynomial for the background. The width of the Gaussian and the shape of the background are determined using the Monte Carlo events. We use a width of 110 MeV for the $\mu^+\mu^-$ channel and 100 MeV for the e^+e^- channel. As can be seen from the figure the shape of the background is well reproduced by the simulation. The scale is left free in the fit, but differs from the absolute prediction by less than 10%. We find 43 ± 8 $J \rightarrow \mu^+\mu^-$ candidates and 15 ± 5 $J \rightarrow e^+e^-$ candidate events over backgrounds of 15 and 5 events, respectively.

The systematic error coming from the fit was estimated by using an exponential function for the background shape, by varying the width of the Gaussian by 10 MeV and by varying the range over which we performed the fit. Leaving the width or the background shape free in the fit, we obtain consistent results, but with larger errors.

The branching ratio $Z^0 \rightarrow J + X$ is calculated as follows:

$$\text{Br}(Z^0 \rightarrow J + X) = \frac{N_J}{\varepsilon_J \cdot \varepsilon_{\ell^+\ell^-}} \cdot \frac{\varepsilon_h}{N_h} \cdot \frac{\Gamma_h}{\Gamma_Z} \cdot \frac{1}{\text{Br}(J \rightarrow \ell^+\ell^-)}$$

where N_J and N_h are the number of the J meson signal events and the total number of hadronic Z^0 decays, respectively, and ε_h is the selection efficiency for hadronic events [10]. ε_J denotes the geometric and kinematic acceptance for the J meson, while $\varepsilon_{\ell^+\ell^-}$ takes into account detector inefficiencies that are not included in the Monte Carlo simulation. Both efficiencies were described in the previous section.

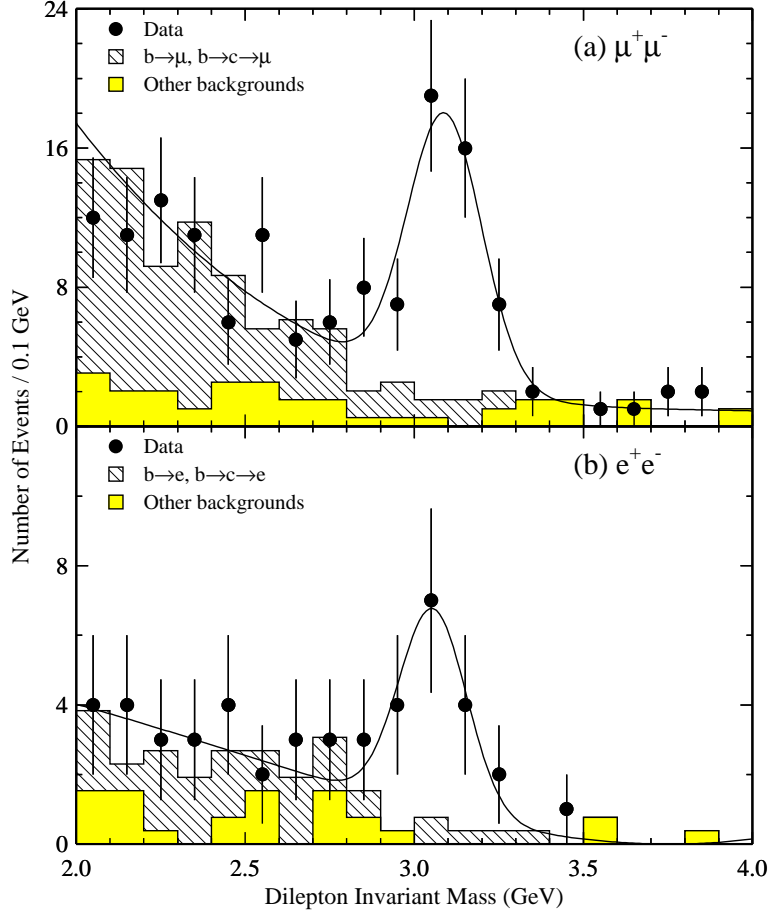


Figure 2: The invariant mass distributions of (a) $\mu^+\mu^-$, and (b) e^+e^- pairs. The curves are the result of the fit described in the text. The contributions from the various backgrounds are shown by the histograms.

Γ_h and Γ_Z are taken from the L3 measurements [10]. We use the recent measurement of $\text{Br}(J \rightarrow \ell^+\ell^-) = 0.0590 \pm 0.0015$ (stat.) ± 0.0019 (sys.) from the MARK-III experiment [18]. We determine:

$$\begin{aligned} \text{Br}(Z^0 \rightarrow J + X) &= (4.5 \pm 0.8 \text{ (stat.)} \pm 0.4 \text{ (sys.)}) \times 10^{-3} \quad \text{from the } \mu^+\mu^- \text{ channel and} \\ \text{Br}(Z^0 \rightarrow J + X) &= (3.5 \pm 1.2 \text{ (stat.)} \pm 0.4 \text{ (sys.)}) \times 10^{-3} \quad \text{from the } e^+e^- \text{ channel.} \end{aligned}$$

Table 1 lists the various contributions to the systematic error on the measurement of the branching ratio $\text{Br}(Z^0 \rightarrow J + X)$. These are added in quadrature to obtain the total systematic error. Combining the two measurements and taking into account the common systematic errors,

we obtain an average branching ratio:

$$\text{Br}(Z^0 \rightarrow J + X) = (4.1 \pm 0.7 \text{ (stat.)} \pm 0.3 \text{ (sys.)}) \times 10^{-3}.$$

This is in good agreement with the other measurement made at LEP [4].

Contribution	$\Delta\text{Br}(Z^0 \rightarrow J + X) \times 10^{-3}$	
	$\mu^+\mu^-$	e^+e^-
Fitting procedure	0.2	0.3
J selection	0.2	0.2
Dimuon detection efficiencies	0.1	—
Dielectron detection efficiencies	—	0.1
$\text{Br}(J \rightarrow \ell^+\ell^-)$	0.2	0.2

Table 1: Contributions to the systematic error on the $\text{Br}(Z^0 \rightarrow J + X)$ measurement, obtained by changing the method or varying the parameters by their errors, as described in the text.

6 Upper Limit on $\text{Br}(Z^0 \rightarrow q\bar{q}g^*; g^* \rightarrow J + X)$

To distinguish the J mesons produced by gluon jets from those coming from the b-hadron decays, we make use of the fact that in the former case the J mesons are expected to be produced at large angles, ϑ_J , with respect to the most energetic quark. We approximate the quark direction by that of the most energetic jet in the event. Figure 3a shows the angular distribution of ϑ_J for the J candidate events in the mass region $2.8 < m_{\ell^+\ell^-} < 3.4$ GeV and for the predicted background. The predicted distributions for $b \rightarrow J + X$ and $g^* \rightarrow J + X$ are shown in Figures 3b and 3c respectively. The angular distribution for Figure 3c is produced using the CORFUJ model [19], in which the excited gluon decays into a J meson and two gluons. The muon and electron samples are combined in these figures. A sample enriched in J particles from gluon jets can be obtained by selecting events in the range $20^\circ < \vartheta_J < 160^\circ$. There are a total of 11 data events in this range. The number of background events predicted by the Monte Carlo is 4, leaving 7 events from gluons or b-decays. This number is small compared with the 59 events obtained without this additional cut, indicating that J production from gluon jets is suppressed.

We set a limit on the production rate from gluon jets by performing a maximum likelihood fit to the ϑ_J distribution over the entire angular range. In the fit we vary the fraction of $g^* \rightarrow J + X$ and $b \rightarrow J + X$. The background contribution is obtained using the five-flavour Monte Carlo events generated with JETSET. The fraction of J mesons coming from gluon jets is determined to be:

$$f_g = 0.03_{-0.06}^{+0.08} \text{ (stat.)} \pm 0.02 \text{ (sys.)}$$

The systematic error comes from the uncertainty in the background contribution.

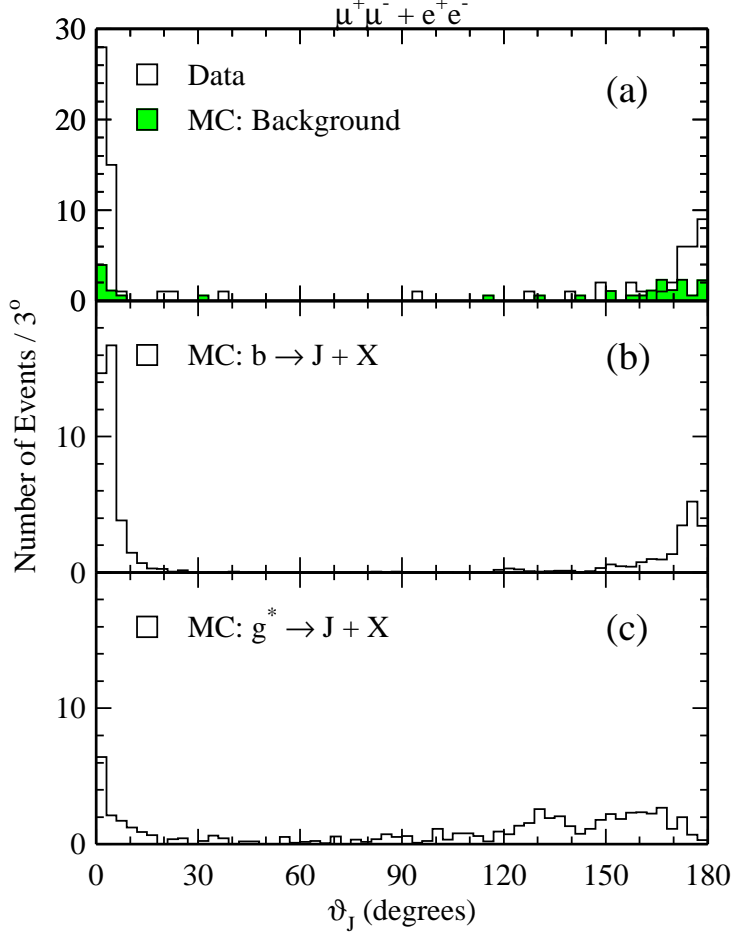


Figure 3: The ϑ_J distributions for (a) the data, and the background as predicted by Monte Carlo; (b) the decay chain $Z^0 \rightarrow b\bar{b}$; $b(\bar{b}) \rightarrow J + X$; $J \rightarrow \ell^+\ell^-$ Monte Carlo simulation; and (c) the decay chain $Z^0 \rightarrow q\bar{q}g^*$; $g^* \rightarrow J + X$; $J \rightarrow \ell^+\ell^-$ as predicted by the CORFUJ model. Figures (b) and (c) are normalized to the number of events in the background-subtracted data.

The acceptance for the decay chain $Z^0 \rightarrow q\bar{q}g^*$; $g^* \rightarrow J + X$; $J \rightarrow \ell^+\ell^-$ is determined to be 0.20 ± 0.01 for $J \rightarrow \mu^+\mu^-$ and 0.12 ± 0.01 for $J \rightarrow e^+e^-$, including all detector efficiencies. Constraining $0 \leq f_g \leq 1$, we set an upper limit of $\text{Br}(Z^0 \rightarrow q\bar{q}g^*; g^* \rightarrow J + X) < 7.0 \times 10^{-4}$ at 90% confidence level.

7 Determination of $\text{Br}(b \rightarrow J + X)$

The branching ratio $\text{Br}(b \rightarrow J + X)$ can be deduced using the following relationship:

$$\text{Br}(b \rightarrow J + X) = \frac{\Gamma_Z}{2 \cdot \Gamma_{b\bar{b}}} \cdot (1 - f_g) \cdot \text{Br}(Z^0 \rightarrow J + X).$$

Using the L3 measurement of Γ_Z [10] and $\Gamma_{b\bar{b}}$ [11], we find

$$\text{Br}(b \rightarrow J + X) = (1.3 \pm 0.2 \text{ (stat.)} \pm 0.2 \text{ (sys.)}) \times 10^{-2}.$$

This branching ratio may be compared with $(1.12 \pm 0.20) \times 10^{-2}$ obtained by experiments at CESR and DORIS [3] for B_u and B_d mesons. Taking into account the different values for $\text{Br}(J \rightarrow \ell^+ \ell^-)$ used in the calculations, the ratio of the two branching ratios is 1.00 ± 0.24 . It should be noted that in addition to the B_u and B_d mesons, B_s and B_c mesons and b-baryons are also produced at LEP. We therefore measure the average branching ratio of $\text{Br}(b \rightarrow J + X)$ weighted by a larger variety of b-hadrons than at CESR and DORIS.

8 Measurement of the b-quark Fragmentation

Given that the J mesons are produced predominantly from the decay of the b-hadrons, the measured J momentum is sensitive to the fragmentation of the b-quark. We can use the J momentum distribution to determine that of the b-quark.

The momentum distributions for the J meson candidates from the $\mu^+ \mu^-$ and $e^+ e^-$ channels in the mass region $2.8 < m_{\ell^+ \ell^-} < 3.4$ GeV are shown in Figure 4. The fraction of the events that are from $b \rightarrow J + X$ is about 75%. The background is dominated by events with one prompt lepton and one from a cascade decay. We perform a binned maximum likelihood fit to the distributions, to extract the Peterson fragmentation parameter [14], ε_b . In the fit, the J momentum distribution and the one due to the cascade decay of the b-hadron are weighted as a function of $x_B \equiv 2E_{\text{hadron}}/\sqrt{s}$ by varying the parameter ε_b , assuming that the x_B distribution can be approximated by the Peterson function (replacing z by x_B). The number of Monte Carlo events is normalized to the number of J candidate events.

The systematic error is estimated by varying background fraction and selection criteria and includes the uncertainty in the fraction of events coming from gluons. We also used the EURODEC [20] package to simulate the weak decay of the b-hadron produced by the JETSET program. The differences in the treatment of the b-hadron decay contributes ± 0.006 to the systematic error on ε_b .

We perform a combined fit using the inclusive $e^+ e^-$ and $\mu^+ \mu^-$ events and obtain:

$$\varepsilon_b = 0.044_{-0.018}^{+0.026} (\text{stat.})_{-0.013}^{+0.009} (\text{sys.}),$$

which corresponds to the average energy fraction of b-hadron:

$$\langle x_B \rangle = 0.70 \pm 0.03 (\text{stat.})_{-0.01}^{+0.02} (\text{sys.}).$$

This measurement is in good agreement with our earlier results on b-quark fragmentation, obtained by a study of the momentum and transverse momentum spectra of inclusive leptons from b-hadron semileptonic decays [11], where we found $\varepsilon_b = 0.050 \pm 0.004 (\text{stat.}) \pm 0.010 (\text{sys.})$.

9 Summary

We have performed a measurement of the production of J mesons using a sample of 410 000 hadronic Z^0 decays. From a study of the invariant mass spectra of muon and electron pairs, we find

$$\text{Br}(Z^0 \rightarrow J + X) = (4.1 \pm 0.7 (\text{stat.}) \pm 0.3 (\text{sys.})) \times 10^{-3}.$$

By studying the angular distribution of the J mesons with respect to most energetic jet, we set an upper limit on J meson production from excited gluons of

$$\text{Br}(Z^0 \rightarrow q\bar{q}g^*; g^* \rightarrow J + X) < 7.0 \times 10^{-4}$$

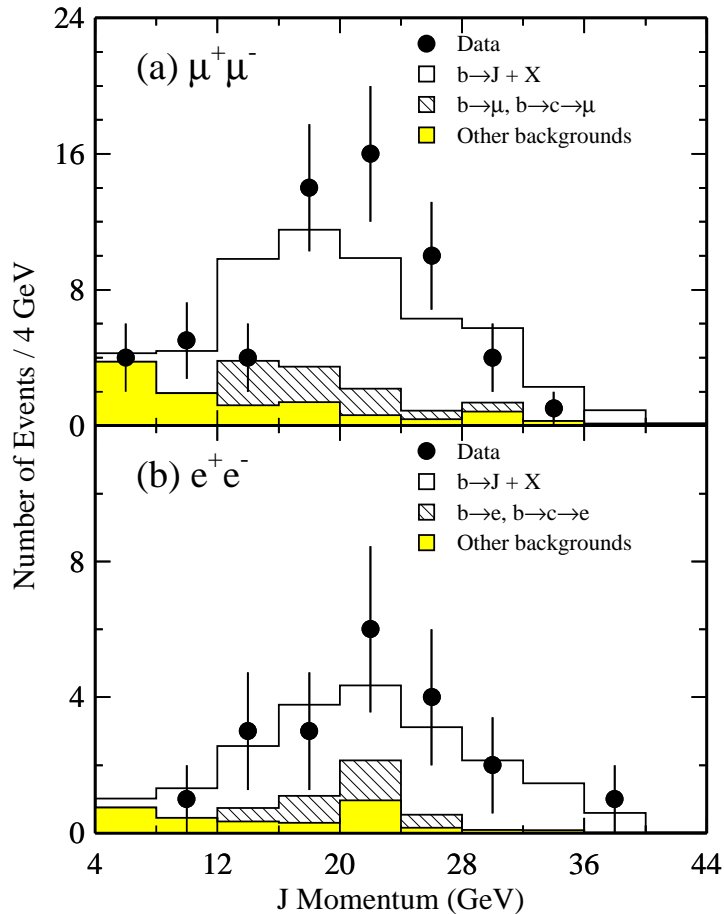


Figure 4: The J momentum distributions from (a) the $\mu^+\mu^-$, and (b) the e^+e^- channels. The fit result and the background contributions are also shown.

at 90% confidence level.

The branching ratio for the production of J mesons from b-quarks, taking into account those coming from gluons, is calculated to be

$$\text{Br}(b \rightarrow J + X) = (1.3 \pm 0.2 (\text{stat.}) \pm 0.2 (\text{sys.})) \times 10^{-2}.$$

From a fit to the momentum distribution of the J meson candidates, the average fractional energy of b-hadrons in $Z^0 \rightarrow b\bar{b}$ decays is determined to be

$$\langle x_B \rangle = 0.70 \pm 0.03 (\text{stat.})_{-0.01}^{+0.02} (\text{sys.}).$$

Acknowledgments

We wish to express our gratitude to the CERN accelerator divisions for the excellent performance of the LEP machine. We acknowledge the contributions of all the engineers and technicians who have participated in the construction and maintenance of this experiment. We would like to thank W.J. Stirling for providing the CORFUJ Monte Carlo program.

References

- [1] J. H. Kühn, S. Nussinov and R. Rückl, *Z. Phys.* **C 5** (1980) 117;
J. H. Kühn and R. Rückl, *Phys. Lett.* **B 135** (1984) 477;
M. B. Wise, *Phys. Lett.* **B 89** (1980) 229;
T. DeGrand and T. Toussaint, *Phys. Lett.* **B 89** (1980) 256;
P. H. Cox *et al.*, *Phys. Rev.* **D 32** (1985) 1157;
I. Bigi and A. Sanda, *Nucl. Phys.* **B 193** (1981) 98.
- [2] H. Fritzsch, *Phys. Lett.* **B 86** (1979) 164, 343.
- [3] CLEO Collaboration, M.S. Alam *et al.*, *Phys. Rev.* **D 34** (1986) 3279;
ARGUS Collaboration, H. Albrecht *et al.*, *Phys. Lett.* **B 199** (1987) 451;
CRYSTAL BALL Collaboration, W. Maschmann *et al.*, *Z. Phys.* **C 46** (1990) 552.
- [4] OPAL Collaboration, G. Alexander *et al.*, *Phys. Lett.* **B 266** (1991) 485.
- [5] G. C. Branco, H. P. Nilles and K. H. Streng, *Phys. Lett.* **B 85** (1979) 269.
- [6] K. Hagiwara, A. D. Martin and W. J. Stirling, *Phys. Lett.* **B 51** (1991) 517.
- [7] B. Guberina, J. H. Kühn, R. D. Peccei and R. Rückl, *Nucl. Phys.* **B 174** (1980) 317.
- [8] L3 Collaboration, B. Adeva *et al.*, *Nucl. Inst. and Meth.* **A289** (1990) 35.
- [9] O. Adriani *et al.*, *Nucl. Inst. and Meth.* **A302** (1991) 53.
- [10] L3 Collaboration, B. Adeva *et al.*, *Z. Phys.* **C 51** (1991) 179.
- [11] L3 Collaboration, B. Adeva *et al.*, *Phys. Lett.* **B 261** (1991) 177.
- [12] T. Sjöstrand and M. Bengtsson, *Comput. Phys. Commun.* **43** (1987) 367;
T. Sjöstrand in “Z Physics at LEP”, CERN Report CERN-89-08, Vol. III, p. 143.
For the 1990 data we used JETSET 7.2 and for the 1991 data we used JETSET 7.3.
- [13] The L3 detector simulation is based on GEANT Version 3.14.
See R. Brun *et al.*, “GEANT 3”, CERN DD/EE/84-1 (Revised), September 1987. Hadronic interactions are simulated using the GHEISHA program; see H. Fesefeldt, RWTH Aachen Report PITHA 85/02 (1985).
- [14] C. Peterson *et al.*, *Phys. Rev.* **D 27** (1983) 105.
- [15] For a compilation of experimental results see: J. Chrin, *Z. Phys.* **C 36** (1987) 163.
- [16] See J.J. Hernández *et al.*, Review of Particle Properties 1990 *Phys. Lett.* **B 239** (1990) 1, page VII.113. We have averaged the PETRA and PEP measurements according to the procedure used by the Particle Data Group.
- [17] ARGUS Collaboration, H. Albrecht *et al.*, *Phys. Lett.* **B 277** (1992) 209.
- [18] MARK-III Collaboration, D. Coffman *et al.*, *Phys. Rev. Lett.* **68** (1992) 282.
- [19] W. J. Stirling, CORFUJ Monte Carlo program, private communication.

- [20] A. Ali and B. van Eijk, in “Z Physics at LEP”, CERN Report CERN-89-08, Vol. III, p. 226.

The L3 Collaboration:

O.Adriani,¹⁴ M.Aguilar-Benitez,²³ S.Ahlen,⁹ H.Akbari,⁵ J.Alcaraz,¹⁵ A.Aloisio,²⁵ G.Alverson,¹⁰ M.G.Alvigi,²⁵ G.Ambrosi,³⁰ Q.An,¹⁶ H.Anderhub,⁴² A.L.Anderson,¹³ V.P.Andreev,³⁴ T.Angelov,¹³ L.Antonov,³⁷ D.Antrasyan,⁷ P.Arce,²³ A.Arefiev,²⁴ A.Atamanchuk,³⁴ T.Azmoon,³ T.Aziz,^{8,1} P.V.K.S.Baba,¹⁶ P.Bagnaia,³³ J.A.Bakken,³² L.Baksay,³⁸ R.C.Ball,³ S.Banerjee,⁸ J.Bao,⁵ R.Barillere,¹⁵ L.Barone,³³ R.Battiston,³⁰ A.Bay,¹⁷ F.Becattini,¹⁴ U.Becker,^{13,42} F.Behner,⁴² J.Behrens,⁴² S.Beingessner,⁴ Gy.L.Bencze,¹¹ J.Berdugo,²³ P.Berges,¹³ B.Bertucci,³⁰ B.L.Betev,^{37,42} M.Biasini,³⁰ A.Biland,⁴² G.M.Bilei,³⁰ R.Bizzarri,³³ J.J.Blaising,⁴ B.Blumenfeld,⁵ G.J.Bobbink,^{15,2} M.Bocciolini,¹⁴ R.Bock,¹ A.Böhm,¹ B.Borgia,³³ D.Bourilkov,²⁷ M.Bourquin,¹⁷ D.Boutigny,⁴ B.Bouwens,² E.Brambilla,²⁵ J.G.Branson,³⁵ I.C.Brock,³¹ M.Brooks,²¹ C.Buisson,²² A.Bujak,³⁹ J.D.Burger,¹³ W.J.Burger,¹⁷ J.P.Burq,²² J.Busenitz,³⁸ X.D.Cai,¹⁶ M.Capell,²⁰ M.Caria,³⁰ G.Carlinio,²⁵ F.Carminati,¹⁴ A.M.Cartacci,¹⁴ M.Cerrada,²³ F.Cesaroni,³³ Y.H.Chang,¹³ U.K.Chaturvedi,⁶ M.Chemarin,²² A.Chen,⁴⁴ C.Chen,⁶ G.M.Chen,⁶ H.F.Chen,¹⁸ H.S.Chen,⁶ J.Chen,¹³ M.Chen,¹³ M.L.Chen,³ W.Y.Chen,¹⁶ G.Chiefari,²⁵ C.Y.Chien,⁵ M.Chmeissani,³ S.Chung,¹³ C.Civinini,¹⁴ I.Clare,¹³ R.Clare,¹³ T.E.Coan,²¹ H.O.Cohn,²⁸ G.Coignet,⁴ N.Colino,¹⁵ A.Contin,⁷ F.Crijns,²⁷ X.T.Cui,¹⁶ X.Y.Cui,¹⁶ T.S.Dai,¹³ R.D'Alessandro,¹⁴ R.de Asmundis,²⁵ A.Degré,⁴ K.Deiters,¹³ E.Dénes,¹¹ P.Denes,³² F.DeNotaristefani,³³ M.Dhina,⁴² D.DiBitonto,³⁸ M.Diomoz,³³ H.R.Dimitrov,³⁷ C.Dionisi,^{33,15} M.T.Dova,¹⁶ E.Drago,²⁵ T.Driever,²⁷ D.Duchesneau,¹⁷ P.Duinker,² H.El Mamouni,²² A.Engler,³¹ F.J.Eppling,¹³ F.C.Erné,² P.Extermann,¹⁷ R.Fabbretti,⁴⁰ M.Fabre,⁴⁰ S.Falciano,³³ S.J.Fan,³⁶ O.Fackler,²⁰ J.Fay,²² M.Felcini,¹⁵ T.Ferguson,³¹ D.Fernandez,²³ G.Fernandez,²³ F.Ferroni,³³ H.Fesefeldt,¹ E.Fiandrini,³⁰ J.Field,¹⁷ F.Filthaut,²⁷ G.Finocchiaro,³³ P.H.Fisher,⁵ G.Forconi,¹⁷ T.Foreman,² K.Freudenreich,⁴² W.Friebe,⁴¹ M.Fukushima,¹³ M.Gailloud,¹⁹ Yu.Galaktionov,^{24,13} E.Gallo,¹⁴ S.N.Ganguli,⁵ P.Garcia-Abia,²³ S.S.Gau,⁴⁴ D.Gele,²² S.Gentile,^{33,15} S.Goldfarb,³ Z.F.Gong,¹⁸ E.Gonzalez,²³ P.Göttlicher,¹ A.Gougas,⁵ D.Goujon,¹⁷ G.Gratta,²⁹ C.Grinnell,¹³ M.Gruenewald,²⁹ C.Gu,¹⁶ M.Guanzioli,¹⁶ J.K.Guo,³⁶ V.K.Gupta,³² A.Gurtu,^{15,8} H.R.Gustafson,³ L.J.Gutay,³⁹ K.Hangarter,¹ A.Hasan,¹⁶ D.Hauschildt,² C.F.He,³⁶ T.Hebbeker,¹ M.Hebert,³⁵ G.Herten,¹³ U.Herten,¹ A.Hervé,¹⁵ K.Hilgers,¹ H.Hofer,⁴² H.Hoorani,¹⁷ G.Hu,¹⁶ G.Q.Hu,³⁶ B.Ille,²² M.M.Ilyas,¹⁶ V.Innocente,^{15,25} H.Janssen,¹⁵ S. Jezequel,⁴ B.N.Jin,⁶ L.W.Jones,³ A.Kasser,¹⁹ R.A.Khan,¹⁶ Yu.Kamyshkov,²⁸ P.Kapinos,^{34,41} J.S.Kapustinsky,²¹ Y.Karyotakis,^{15,4} M.Kaur,¹⁶ S.Khokhar,¹⁶ M.N.Kienzle-Focacci,¹⁷ W.W.Kinnison,²¹ D.Kirkby,²⁹ S.Kirsch,⁴¹ W.Kittel,²⁷ A.Klimentov,^{13,24} A.C.König,²⁷ E.Koffeman,² O.Kornadt,¹ V.Koutsenko,^{13,24} A.Koulbaridis,³⁴ R.W.Kraemer,³¹ T.Kramer,¹³ V.R.Krastev,^{37,30} W.Krenz,¹ A.Krivshich,³⁴ H.Kuitjen,²⁷ K.S.Kumar,¹² A.Kunin,^{10,24} G.Landi,⁴ D.Lanske,¹ S.Lanzano,²⁵ P.Lebrun,²² P.Lecomte,⁴² P.Lecoq,¹⁵ P.Le Coultre,⁴² D.M.Lee,²¹ I.Leedom,¹⁰ J.M.Le Goff,¹⁵ R.Leiste,⁴¹ M.Lenti,¹⁴ E.Leonardi,³³ J.Letry,⁴² X.Leytens,² C.Li,^{8,16} H.T.Li,³⁶ P.J.Li,³⁶ X.G.Li,⁶ J.Y.Liao,³⁶ W.T.Lin,⁴⁴ Z.Y.Lin,¹⁸ F.L.Linde,^{15,2} B.Lindemann,¹ D.Linnhofer,⁴² L.Lista,²⁵ Y.Liu,¹⁶ W.Lohmann,^{41,15} E.Longo,³³ Y.S.Lu,⁶ J.M.Lubbers,¹⁵ K.Lübelsmeyer,¹ C.Luci,³³ D.Luckey,^{7,13} L.Ludovici,³³ L.Luminari,³³ W.G.Ma,¹⁸ M.MacDermott,⁴² P.K.Malhotra,^{8,1} R.Malik,⁶ A.Malinin,^{4,24} C.Maña,²³ D.N.Mao,³ Y.F.Mao,⁶ M.Maolinbay,⁴² P.Marchesini,⁴² F.Marion,⁴ A.Marin,⁹ J.P.Martin,²² L.Martinez-Laso,²³ F.Marzano,³³ G.G.Massarò,² T.Matsuda,¹³ K.Mazumdar,⁸ P.McBride,¹² T.McMahon,³⁹ D.McNally,⁴² Th.Meinholtz,¹ M.Merk,²⁷ L.Merola,²⁵ M.Meschini,⁴ W.J.Metzger,²⁷ Y.Mi,¹⁶ G.B.Mills,²¹ Y.Mir,¹⁶ G.Mirabelli,³³ J.Mnich,¹ M.Möller,¹ B.Monteleoni,¹⁴ R.Morand,⁴ S.Morganti,³³ N.E.Moulai,¹⁶ R.Mount,²⁹ S.Müller,¹ A.Nadtochy,³⁴ E.Nagy,¹¹ M.Napolitano,²⁵ H.Newman,²⁹ C.Neyer,⁴² M.A.Niaz,¹⁶ A.Nippe,¹ H.Nowak,⁴¹ G.Organtini,³³ D.Pandoulas,¹ S.Paoletti,¹⁴ P.Paolucci,²⁵ G.Passaleva,^{14,30} S.Patricelli,²⁵ T.Paul,⁵ M.Pauluzzi,³⁰ F.Pauss,⁴² Y.J.Pei,¹ D.Perret-Gallix,⁴ J.Perrier,¹⁷ A.Pevsner,⁵ D.Piccolo,²⁵ M.Pieri,^{15,14} P.A.Piroué,³² F.Plasil,²⁸ V.Plyaskin,²⁴ M.Pohl,⁴² V.Pojidaev,^{24,14} N.Produit,¹⁷ J.M.Qian,³ K.N.Qureshi,¹⁶ R.Raghavan,⁸ G.Rahal-Callot,⁴² G.Raven,² P.Razis,²⁶ K.Read,²⁸ D.Ren,⁴² Z.Ren,¹⁶ M.Rescigno,³³ S.Reucroft,⁰ A.Ricker,¹ S.Riemann,⁴¹ O.Rind,³ H.A.Rizvi,¹⁶ F.J.Rodriguez,²³ B.P.Roe,³ M.Röhner,¹ S.Röhner,¹ L.Romero,²³ J.Rose,¹ S.Rosier-Lees,⁴ R.Rosmalen,²⁷ Ph.Rosset,¹⁹ A.Rubbia,¹³ J.A.Rubio,¹⁵ H.Rykaczewski,⁴² M.Sachwitz,⁴¹ E.Sajan,³⁰ J.Salicio,¹⁵ J.M.Salicio,²³ G.S.Sanders,²¹ A.Santocchia,³⁰ M.S.Sarakinos,¹³ G.Sartorelli,^{7,16} M.Sassowsky,¹ G.Sauvage,⁴ V.Schegelsky,³⁴ K.Schmiemann,¹ D.Schmitz,¹ P.Schmitz,¹ M.Schneegans,⁴ H.Schopper,⁴³ D.J.Schotanus,²⁷ S.Shotkin,¹³ H.J.Schreiber,⁴¹ J.Shukla,³¹ R.Schulte,¹ S.Schulte,¹ K.Schultze,¹² J.Schütte,¹² J.Schwenke,¹ G.Schwering,¹ C.Sciacca,²⁵ I.Scott,¹² R.Sehgal,¹⁶ P.G.Seiler,⁴⁰ J.C.Sens,^{15,2} L.Servoli,³⁰ I.Sheer,³⁵ D.Z.Shen,³⁶ S.Shevchenko,²⁹ X.R.Shi,²⁹ E.Shumilov,²⁴ V.Shoutko,²⁴ E.Soderstrom,³² A.Sopczak,³⁵ C.Spartiotis,⁵ T.Spickermann,¹ P.Spillantini,¹⁴ R.Starosta,¹ M.Steuer,^{7,13} D.P.Stickland,³² F.Sticozzi,¹³ H.Stone,¹⁷ K.Strauch,¹² B.C.Stringfellow,³⁹ K.Sudhakar,^{8,1} G.Sultanov,¹⁶ R.L.Sumner,³² L.Z.Sun,^{18,16} H.Suter,⁴² R.B.Sutton,³¹ J.D.Swain,¹⁶ A.A.Syed,¹⁶ X.W.Tang,⁶ L.Taylor,¹⁰ C.Timmermans,²⁷ Samuel C.C.Ting,¹³ S.M.Ting,¹³ M.Tonutti,¹ S.C.Tonwar,⁸ J.Tóth,¹¹ A.Tsaregorodtsev,³⁴ G.Tsipolitis,³¹ C.Tully,²⁹ K.L.Tung,⁶ J.Ulbricht,⁴² L.Urbán,¹¹ U.Uwer,¹ E.Valente,³³ R.T.Van de Walle,²⁷ I.Vetlitsky,²⁴ G.Viertel,⁴² P.Vikas,¹⁶ U.Vikas,¹⁶ M.Vivargent,⁴ H.Vogel,³¹ H.Vogt,⁴¹ I.Vorobiev,²⁴ A.A.Vorobyov,³⁴ L.Vuilleumier,¹⁹ M.Wadhwa,¹⁶ W.Wallraff,¹ C.R.Wang,¹⁸ G.H.Wang,³¹ J.H.Wang,⁶ Q.F.Wang,¹² X.L.Wang,¹⁸ Y.F.Wang,¹⁴ Z.M.Wang,^{16,18} A.Weber,¹ J.Weber,⁴² R.Weill,⁹ T.J.Wenaus,²⁰ J.Wenninger,¹⁷ M.White,¹³ C.Willmott,²³ F.Wittgenstein,¹⁵ D.Wright,³² R.J.Wu,⁶ S.X.Wu,¹⁶ Y.G.Wu,⁶ B.Wysłouch,¹³ Y.Y.Xie,³⁶ Y.D.Xu,⁶ Z.Z.Xu,¹⁸ Z.L.Xue,³⁶ D.S.Yan,³⁶ X.J.Yan,¹³ B.Z.Yang,¹⁸ C.G.Yang,⁶ G.Yang,¹⁶ K.S.Yang,⁶ Q.Y.Yang,⁶ Z.Q.Yang,³⁶ C.H.Ye,¹⁶ J.B.Ye,¹⁸ Q.Ye,¹⁶ S.C.Yeh,⁴⁴ Z.W.Yin,³⁶ J.M.You,¹⁶ N.Yunus,¹⁶ M.Yzerman,² C.Zaccardelli,²⁹ P.Zemp,⁴² M.Zeng,¹⁶ Y.Zeng,¹ D.H.Zhang,² Z.P.Zhang,^{18,16} B.Zhou,⁹ J.F.Zhou,¹ R.Y.Zhu,²⁹ H.L.Zhuang,⁶ A.Zichichi,^{7,15,16} B.C.C.van der Zwaan,²

-
- 1 I. Physikalisches Institut, RWTH, W-5100 Aachen, FRG[§]
 - III. Physikalisches Institut, RWTH, W-5100 Aachen, FRG[§]
 - 2 National Institute for High Energy Physics, NIKHEF, NL-1009 DB Amsterdam, The Netherlands
 - 3 University of Michigan, Ann Arbor, MI 48109, USA
 - 4 Laboratoire de Physique des Particules, LAPP, F-74941 Annecy-le-Vieux, France
 - 5 Johns Hopkins University, Baltimore, MD 21218, USA
 - 6 Institute of High Energy Physics, IHEP, Beijing, P.R. China
 - 7 INFN-Sezione di Bologna, I-40126 Bologna, Italy
 - 8 Tata Institute of Fundamental Research, Bombay 400 005, India
 - 9 Boston University, Boston, MA 02215, USA
 - 10 Northeastern University, Boston, MA 02115, USA
 - 11 Central Research Institute for Physics of the Hungarian Academy of Sciences, H-1525 Budapest 114, Hungary
 - 12 Harvard University, Cambridge, MA 02139, USA
 - 13 Massachusetts Institute of Technology, Cambridge, MA 02139, USA
 - 14 INFN Sezione di Firenze and University of Florence, I-50125 Florence, Italy
 - 15 European Laboratory for Particle Physics, CERN, CH-1211 Geneva 23, Switzerland
 - 16 World Laboratory, FBLJA Project, CH-1211 Geneva 23, Switzerland
 - 17 University of Geneva, CH-1211 Geneva 4, Switzerland
 - 18 Chinese University of Science and Technology, USTC, Hefei, Anhui 230 029, P.R. China
 - 19 University of Lausanne, CH-1015 Lausanne, Switzerland
 - 20 Lawrence Livermore National Laboratory, Livermore, CA 94550, USA
 - 21 Los Alamos National Laboratory, Los Alamos, NM 87544, USA
 - 22 Institut de Physique Nucléaire de Lyon, IN2P3-CNRS/Université Claude Bernard, F-69622 Villeurbanne Cedex, France
 - 23 Centro de Investigaciones Energeticas, Medioambientales y Tecnológicas, CIEMAT, E-28040 Madrid, Spain
 - 24 Institute of Theoretical and Experimental Physics, ITEP, Moscow, Russia
 - 25 INFN-Sezione di Napoli and University of Naples, I-80125 Naples, Italy
 - 26 Department of Natural Sciences, University of Cyprus, Nicosia, Cyprus
 - 27 University of Nymegen and NIKHEF, NL-6525 ED Nymegen, The Netherlands
 - 28 Oak Ridge National Laboratory, Oak Ridge, TN 37831, USA
 - 29 California Institute of Technology, Pasadena, CA 91125, USA
 - 30 INFN-Sezione di Perugia and Università Degli Studi di Perugia, I-06100 Perugia, Italy
 - 31 Carnegie Mellon University, Pittsburgh, PA 15213, USA
 - 32 Princeton University, Princeton, NJ 08544, USA
 - 33 INFN-Sezione di Roma and University of Rome, "La Sapienza", I-00185 Rome, Italy
 - 34 Nuclear Physics Institute, St. Petersburg, Russia
 - 35 University of California, San Diego, CA 92182, USA
 - 36 Shanghai Institute of Ceramics, SIC, Shanghai, P.R. China
 - 37 Bulgarian Academy of Sciences, Institute of Mechatronics, BU-1113 Sofia, Bulgaria
 - 38 University of Alabama, Tuscaloosa, AL 35486, USA
 - 39 Purdue University, West Lafayette, IN 47907, USA
 - 40 Paul Scherrer Institut, PSI, CH-5232 Villigen, Switzerland
 - 41 DESY-Institut für Hochenergiephysik, O-1615 Zeuthen, FRG
 - 42 Eidgenössische Technische Hochschule, ETH Zürich, CH-8093 Zürich, Switzerland
 - 43 University of Hamburg, W-2000 Hamburg, FRG
 - 44 High Energy Physics Group, Taiwan, ROC

§ Supported by the German Bundesministerium für Forschung und Technologie

† Deceased.